

Mapping Wind Erosion Susceptibility and Land Degradation Priority Areas Using GIS and Remote Sensing in Semi-Arid Northeastern Algeria

Sara Hassad^{*1,2}, Oussama Meghithi¹, Toufik Aliat^{1,2}, Sarra Boughaba^{1,2}, Nadhir Laouar^{1,2}, Abdelhafid Bouzekri^{1,2}, Chemseddine Fehdi³

¹ Higher National School of Forests, 40000 Khenchela, Algeria.

² Laboratory of Algerian Forests and Climate Change, Higher National School of Forests, 40000 Khenchela, Algeria.

³ Department of Earth Sciences, University of Larbi Tebessi, 12000 Tebessa, Algeria.

*Corresponding author: hassad.sara@ensf.dz

ARTICLE INFO

Received: 15 Aug 2025
Revised: 25 Jan 2026
Accepted: 03 Feb 2026
Published: 08 March 2026

ABSTRACT

Wind erosion is an important factor in land degradation in arid and semi-arid areas, especially in regions with high wind speed, weak soil cohesion, and limited vegetation cover. This research evaluated the susceptibility of wind erosion in the Nemamcha area (Southern part of the Province of Khenchela in northeastern Algeria) using a combination of remote sensing data, climate parameters, soil data, topographic factors, and human-induced factors in a GIS platform based on the weighted multi-attribute approach. Vegetation protection was considered using the Normalized Difference Vegetation Index obtained from Landsat-8 satellite images, while soil and soil surface characteristics were accounted for using land cover types, soil type and classification, soil texture, grain size index, soil moisture index, geology, slope elevation, wind speed values, human pressure, and road network density. Lastly, the map of susceptibility was classified into five susceptibility levels (very low to very high). It was revealed that the high and very high levels of susceptibility cover approximately 58.29% and 24.62% of the area of interest, while the medium susceptibility level is around 11.12%, and the areas classified as low and very low only account for 5.97%. It was noted that the areas of high susceptibility generally correspond to sandy soils and sparse vegetation cover.

Keywords: Geographic Information System, Khenchela, Land degradation, Remote sensing, Vegetation cover, Wind erosion.

1. Introduction

Wind erosion represents one of the principal geomorphic processes acting in arid and semi-arid biomes. In addition to the loss of nutrient-rich topsoil, it increases the degradation of the soil itself by reducing fertility, speeding the process of desertification, and increasing dust emission, which negatively affects air quality and human health (Lal, 2003; Ravi et al., 2010). Wind erosion processes and intensity are influenced by the wind conditions and surface properties such as textural class, aggregation, moisture, roughness, and cover (Sterk, 2003; Okin et al., 2006). The growing arid conditions and the increasing pressure on forage range resources have increased the sensitivity of the Mediterranean landscape, especially in the steppe and pre-Saharan areas where the vegetation cover can be patchy and the crusts are weak (Fenta et al., 2020).

Engineering contributions of this work include: (I) a reproducible GIS-based workflow for wind erosion susceptibility mapping using heterogeneous datasets; (II) decision-support outputs that delineate and rank priority intervention zones; and (III) robustness checks based on qualitative sensitivity testing and consistency-based validation.

Remote sensing and Geographic Information Systems (GIS) are efficient methods of wind erosion vulnerability assessment on a regional level. They are able to monitor land cover and vegetation measures uniformly and can combine different data into a single decision-support system (Malczewski, 2006; Elyagoubi and Mezrhab, 2022). Recent studies indicate that wind erosion hotspots can successfully be identified and remediated on a land management level with the help of GIS systems and multicriteria methods (Mihi and Benaradj, 2022; Funk and Völker, 2024).

2. Materials and methods

2.1 Methodological framework

This study adopts the methodological framework of integrating concepts of wind erosion equations within a Geographic Information System to derive a spatial susceptibility. Climatic, soil, topographic, and land-use datasets were elaborated from several sources and harmonized in a GIS environment by using widely adopted GIS-based multi-criteria decision analysis procedures (Malczewski, 2006). The climatic erosivity was estimated from meteorological records, while vegetation cover was analyzed in terms of NDVI from Landsat 8 OLI imagery since this remains a strong estimator of vegetation density and ground surface protection in drylands (Tucker, 1979; Okin et al., 2006).

A GIS-based multi-criteria integration was then applied to combine key controlling factors such as soil erodibility, wind speed, slope conditions, and land cover into a composite wind erosion sensitivity map. This is in concert with the recent application of remote sensing and GIS for mapping wind erosion hazard in semi-arid environments (Elyagoubi and Mezrhab, 2022; Mihi and Benaradj, 2022).

Additionally, the proposed modeling approach is grounded in conventional wind erosion models such as the Wind Erosion Prediction System (WEPS), allowing the assessment of wind erosion processes in a physically proper manner, depending on the environmental conditions (Hagen, 2004). In general, the developed procedure benefits from the current state of the art in terms of the significance of environmental factors in modeling wind erosion (Ghosal and Das Bhattacharya, 2020; Funk and Völker, 2024).

2.2 Robustness checks (engineering decision-support)

To strengthen the operational reliability of the susceptibility mapping workflow, robustness checks were incorporated. A qualitative sensitivity analysis was performed by testing alternative parameter-influence scenarios (e.g., increased influence of vegetation protection and wind forcing) and assessing the stability of high and very high susceptibility zones through map overlays and class-area statistics.

In addition, a consistency-based validation was conducted by comparing the spatial distribution of susceptibility classes with independent evidence of surface exposure (e.g., land-cover patterns indicating bare soil and sparse vegetation) and with expected gradients relative to vegetation density and soil texture. These checks support the use of the resulting map as a decision-support product for mitigation prioritization.

2.3 Implementation and reproducibility

All criteria layers were standardized to a common spatial resolution and coordinate reference system, normalized to comparable scales, and integrated within a GIS environment using a multiplicative combination workflow. The full processing chain (data preparation, normalization, weighting, aggregation, reclassification, and map production) was implemented in a reproducible manner using standard GIS tools, enabling straightforward transfer to comparable semi-arid regions.

2.4 Study area

The study area is situated in the Nemamcha region (southern part of Khenchela Province, northeastern Algeria), characterized by a semi-arid to arid climate with frequent strong winds and landscapes dominated by steppe rangelands, bare soil surfaces, and sandy to calcareous substrates. The total mapped area is around 629,564 ha. (Figure 1).

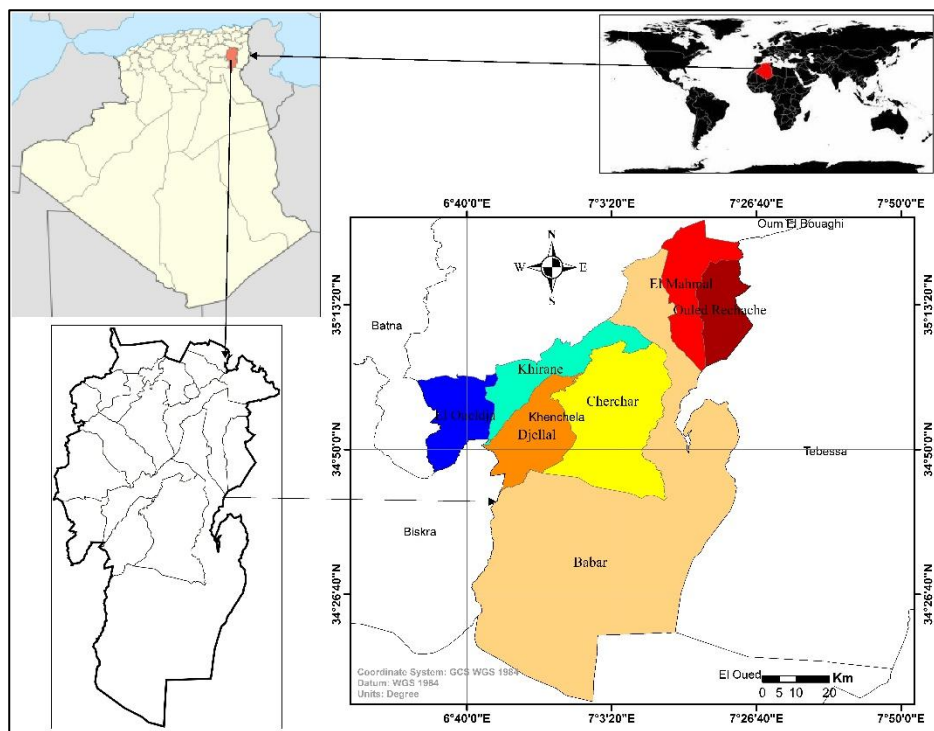


Figure 1. Geographic location and administrative boundaries of the study area.

2.5 Wind erosion model

For the purpose of mapping wind erosion susceptibility, a wind erosion modeling framework was implemented in which sediment detachment and transport are controlled by both climatic forcing and land-surface conditions. Environmental and human-related parameters were extracted from remote sensing and GIS-based thematic layers and then integrated spatially to quantify wind erosion risk across the study area. This GIS-based approach enables the generation of continuous susceptibility maps and supports spatial decision-making for land degradation mitigation (Malczewski, 2006; Funk and Völker, 2024). The overall workflow is consistent with recent studies emphasizing the importance of combining erosion modelling concepts with GIS and remote sensing indicators for regional wind erosion risk mapping (Ghosal and Das Bhattacharya, 2020; Mihi and Benaradj, 2022).

The equation used is:

$$E = N \times C \times L \times P \times T \times S \times Co \times M \times R \times G \times (1/10) \quad \text{Eq. (1)}$$

Where:

E = Wind Erosion Susceptibility Index (WESI)

N = Normalized Difference Vegetation Index (NDVI)

C = Soil classification

L = Lithology

P = Population

- T = Soil texture of the study area
- S = Wind speed
- Co = Land cover
- M = Soil moisture index
- R = Road density
- G = Grain size index

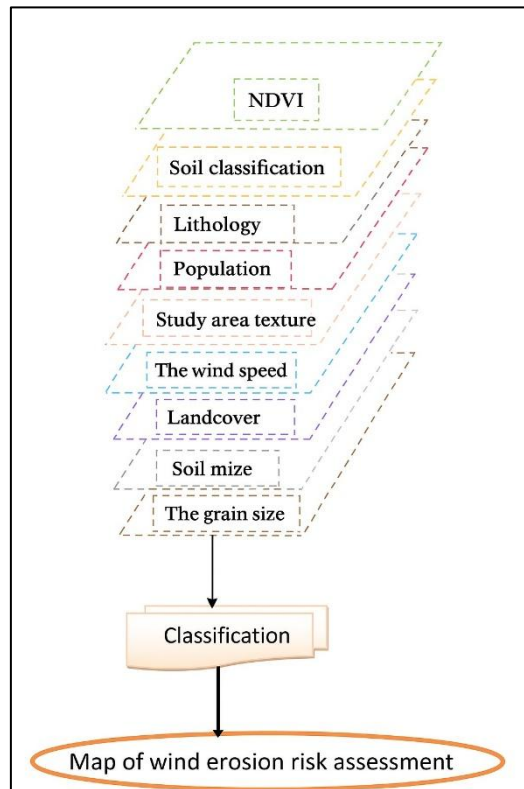


Figure 2. Methodological flowchart.

2.6 Evaluation criteria

2.6.1 Land cover

The land-cover map was produced from a Landsat 8 OLI image using a supervised classification technique that incorporates the maximum likelihood algorithm, which is also a commonly used technique for thematic mapping of land surfaces from multiband satellite images (Pal & Mather, 2003; Roy et al., 2014). The use of false-color composites was helpful for training data sampling and stratification of vegetation, bare surfaces, and urbanized surfaces. Validation of the classification was done by comparing the classification with field GPS data observations, according to principles of accuracy assessment for land classification mapping that are commonly accepted in remote sensing applications (Congalton, 1991; Foody, 2002). The land-cover map includes several classes of land surfaces, including tree crops, market gardens, urban surfaces, forest/maquis/reforestation, field crops under irrigation and rainfed, olive groves, palm groves, water surfaces, polyculture surfaces, surfaces of sand, coarse-textured surfaces, and bare surfaces/rocky outcrops. (Figure 3).

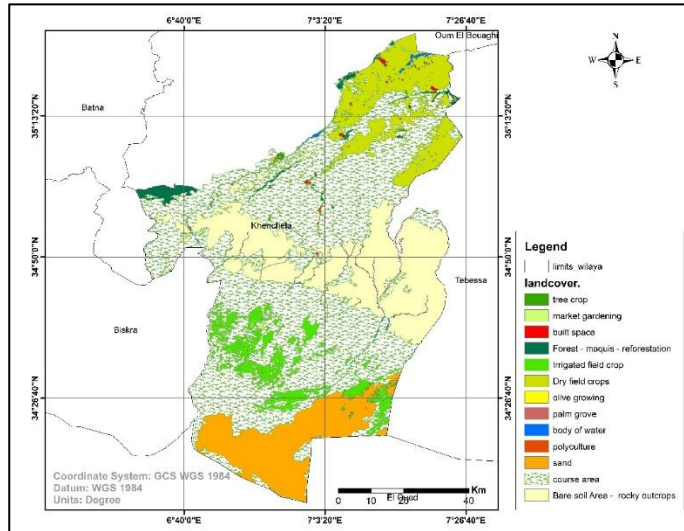


Figure 3. Land cover map.

2.6.2 Vegetation cover (NDVI)

To determine vegetation cover, the Normalized Difference Vegetation Index (NDVI) was calculated using Landsat 8 OLI images, which have been found to be reliable proxies in arid regions (Tucker, 1979; Pettorelli et al., 2005; Roy et al., 2014). NDVI was calculated from Landsat 8 OLI images by using the red band and the near-infrared (NIR) band through the equation:

$$NDVI = (NIR - RED) / (NIR + RED) \quad (Eq. 2)$$

where NIR and RED are the near-infrared and red bands, respectively.

NDVI is employed to quantify spatial variations in vegetation density and condition across the study area. NDVI values indicate regions with dense and strong vegetation; thus, those regions receive increased surface protection against wind action, while low values indicate sparse or degraded surfaces with low protective cover (Tucker, 1979; Okin et al., 2006). In light of this observation, the NDVI map lays a platform for vegetation spatial distribution; therefore, regions that are prone to wind erosion are readily identified based on low plant density (Ravi et al., 2010; Mihi and Benaradj, 2022). (Figure 4).

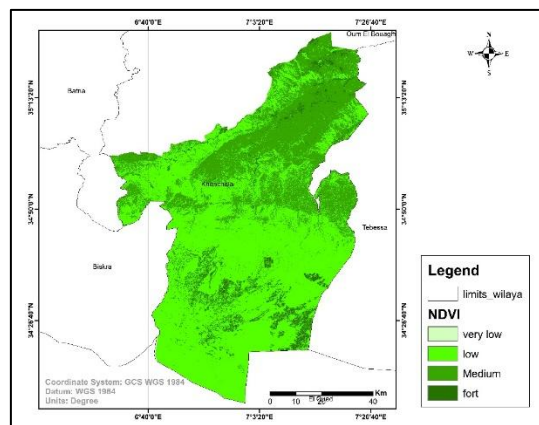


Figure 4. Vegetation cover map.

2.6.3 Grain size index (GSI)

The GSI map was produced for southern Khenchela by incorporating the spatial soil texture information-sand, Sand, silt, and clay fractions were examined in a GIS environment to understand the variability of the surface material in different land-use conditions, such as agricultural, planning, and engineering regions. Texture types were classified depending on the relative distribution of the sand, silt, and clay fractions to identify the dominant types and the possible implications of the texture types in wind erosion susceptibility. Its rationale is supported because soil texture is a significant factor in wind erodibility, in that sandy and loam soils are more likely to have a larger wind-erodible fraction and have stronger susceptibility to soil detachment and transport through strong wind forcing (Colazo and Buschiazzo, 2015; Bouajila et al., 2022).

Consequently, the map shows the predominance of sandy and loamy textures, presumably reflecting enhanced erodibility and increased wind erosion potential in exposed areas with limited surface cohesion (Colazo and Buschiazzo 2015; Rezaei et al. 2022). (Figure 5).

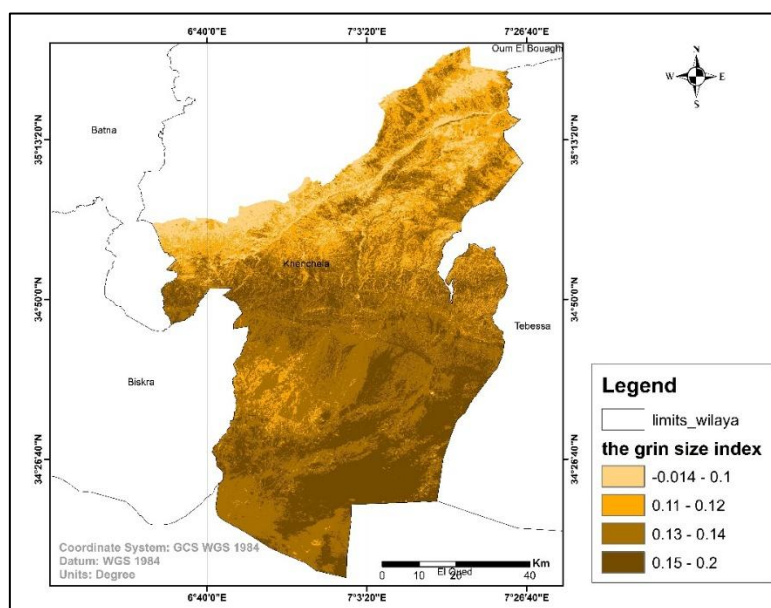


Figure 5. Grain size index map.

2.6.4 Normalized Difference Moisture Index (NDMI)

The soil moisture index map of southern Khenchela has been produced through remote sensing and GIS spatial analysis to identify the distribution of surface moisture conditions in the study area. Landsat 8 OLI satellite images were applied to produce the relative variations in surface moisture through differences in spectral reflectances in the near infrared and shortwave infrared regions, which are sensitive to water in vegetation and surface substances (Gao, 1996; Fensholt and Sandholt, 2003). The formula to determine the moisture index is as follows:

$$\text{NDMI} = (\text{NIR} - \text{SWIR}) / (\text{NIR} + \text{SWIR}) \quad (\text{Eq. 3})$$

The merits of this are that it assists in revealing areas of variation in moisture retention properties, which are mainly a result of topography and vegetation cover and/or irrigation. The areas with low values of a moisture index are mostly exposed areas and rock plains that lack cohesion and predisposed to wind erosion, as compared to uplands and vegetated areas with a relatively high value of a moisture index that are less susceptible to wind erosion due to their ability to protect sediment from being ripped off by wind (Okin et al., 2006; Ravi et al., 2010; Mihi and Benaradj, 2022). (Figure 6).

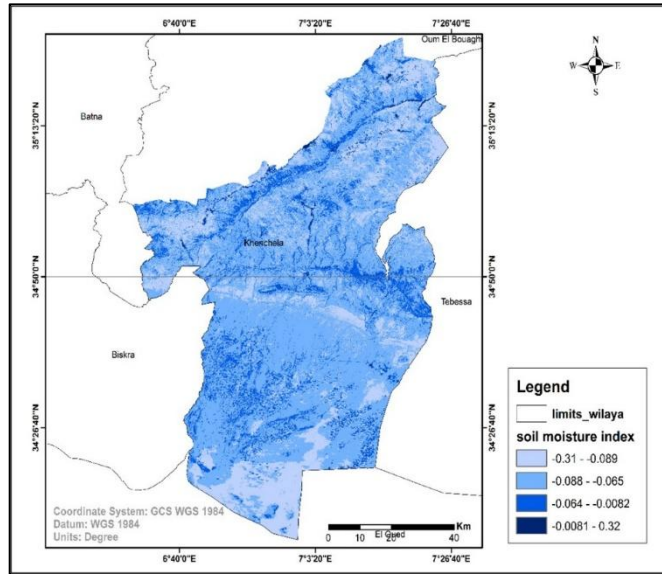


Figure 6. Soil moisture index map.

2.6.5 Soil texture

Soil texture was also examined to determine the amount of sand, silt, and clay percentages at each point of interest in the area, as well as its effect on the susceptibility of the soil to erosion by the action of the wind. Information obtained was analyzed and rendered spatially using a GIS setup, creating a soil texture map. Four main soil textures were shown, which included loamy soil, silt soil, sandy soil, and clay soil. Mapped soil textures were interpreted through their physical properties as well as their response to the detachment of soil particles through the action of the wind. Where soil textures are coarse, as with sandy soil, the soil tends to be more susceptible to erosion as a result of a lack of aggregation while having little cohesion between particles, which makes the particles easy to be moved or transported through erosion (Lyles et al., 1986; Sterk, 2003). Figure 7 shows the spatial representation of soil textures at Khenchela.

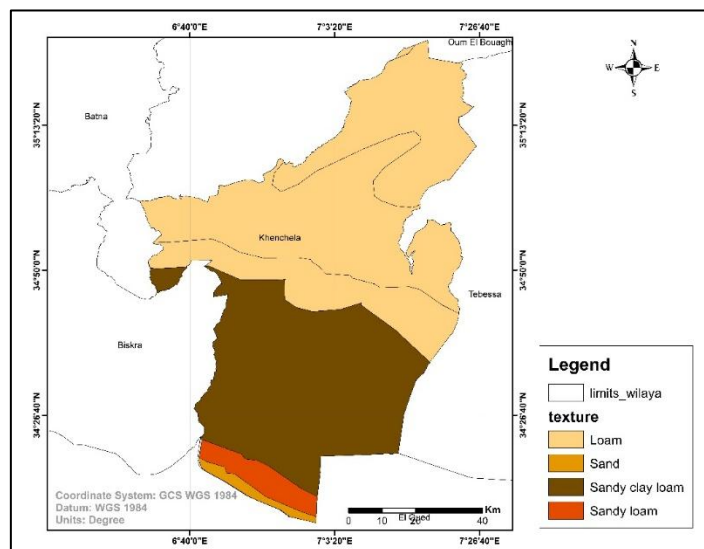


Figure 7. Soil texture map.

2.6.6 Soil type

Soil types in the study area were identified based on field observations and the interpretation of available pedological information. Soil development in southern Khenchela is strongly influenced by parent material, geomorphological units, and the prevailing semi-arid climate. In this context, aeolian and alluvial deposits play a key role in shaping soil properties and spatial variability. Similar patterns of soil–landscape relationships and the occurrence of aeolian-derived soils in arid to semi-arid environments have been reported in regional digital soil mapping studies conducted in Algeria (Assami and Hamdi-Aissa, 2019) and in semi-arid watersheds where soil salinity and substrate variability were mapped using GIS approaches (Djilali et al., 2016). These soil units were mapped in GIS to visualize their spatial distribution and to evaluate their relative susceptibility to wind erosion (Figure 8).

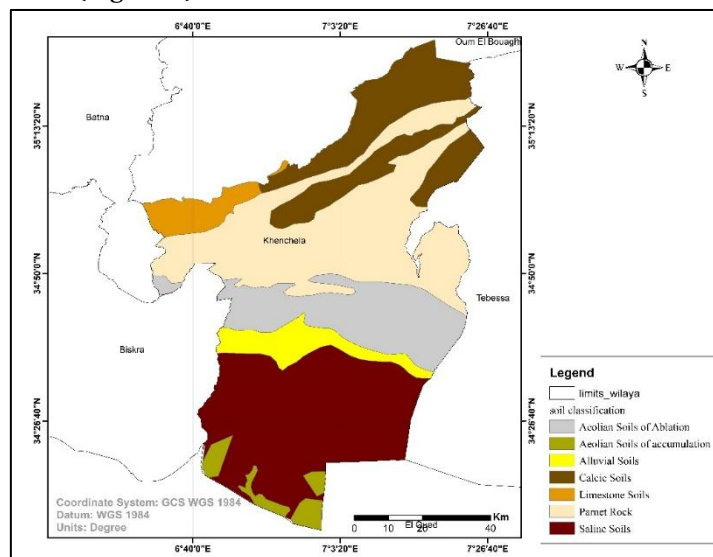


Figure 8. Soil type map.

2.6.7 Lithology

The lithological map of southern Khenchela was generated after compiling available lithological data, digitizing the dominant geological units, as well as creating a GIS environment. Based on the lithological units identified, lithological formations were classified into three groups based upon their susceptibility to erosion, with highly resistant, moderately resistant, and susceptible substrates identified, as susceptibility classes often follow a pattern where the substrate directly influences soil formation, stability, and susceptibility (Djeddaoui et al., 2017). Field data as well as soil data available was also considered for better definition of lithological boundaries as well as for better interpretation of dominant lithological units identified during data analysis. Following the analysis, lithological units were transformed into a raster format map with assigned values for interpretation of their effects upon soil erosion susceptibility as well as wind erosion susceptibility within the multicriteria analysis framework (Malczewski, 2006; Elyagoubi and Mezrhab, 2022). Distribution of lithological units throughout the study area is shown in (Figure 9).

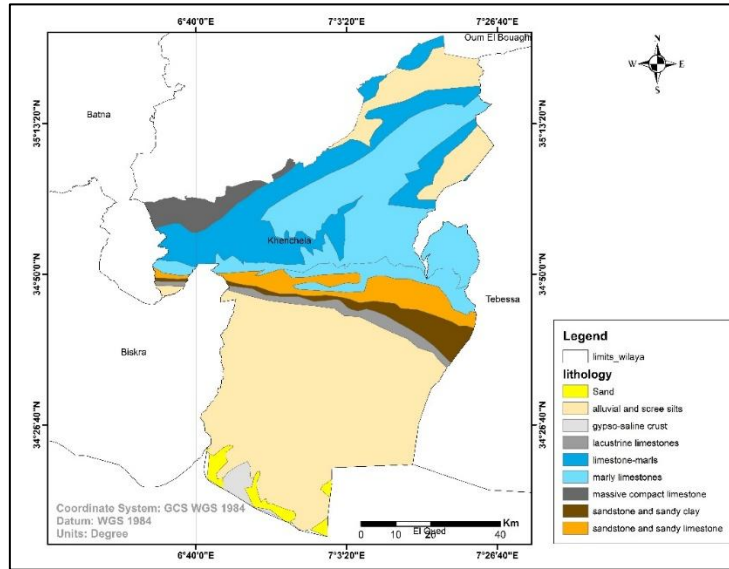


Figure 9. Lithological map.

2.6.8 Slope

Slope map of the area of Khenchela was derived through Digital Elevation Model (DEM). Slope percentage is the ratio of the height of the ground to the distance of the ground and was divided into several classes, which range from flat ground (0-3%) to very steep ground (>30%), as proposed by Warren et al. (2004) and Wechsler (2006). Khenchela province has its steep slopes, particularly within the Aurès and Nemamcha mountain chains, while the Oued Abiod depression and the surrounding regions show gentle slopes with stable topography. SLOPE was used as a criterion for evaluating the risk of wind erosion since it affects near-surface wind dynamics (Okin et al., 2006; Smyth et al., 2019). (Figure 10).

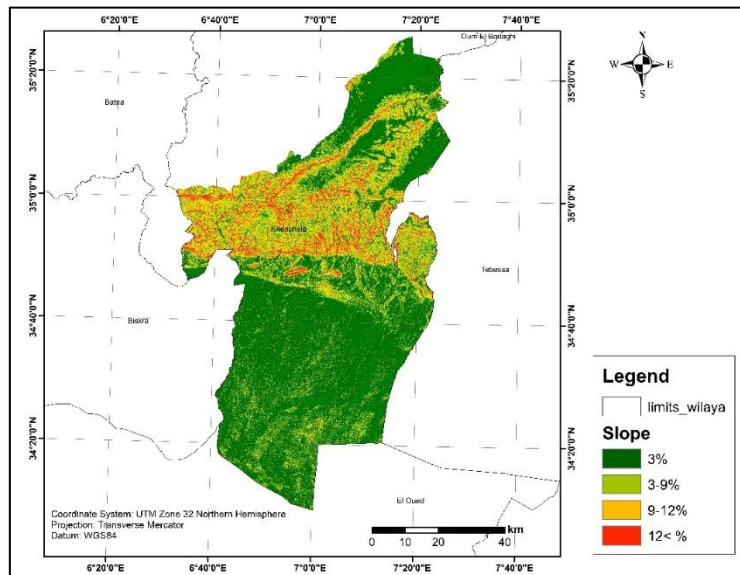


Figure 10. Slope map.

2.6.9 Wind speed

Wind velocity data derived from regional meteorological stations were integrated into the GIS database and used to describe the spatial variation of wind intensity throughout southern Khenchela. Multi-annual averages

were computed to approximate the dominant wind conditions and smooth out short-term temporal variations. The observed velocities in general typically fell between 10 and 30 km h⁻¹. Higher values are concentrated within the southwestern part of the Wilaya, while the lowest values tend towards the northeastern areas. This was followed by a wind speed continuous surface that was able to be created through the use of a spatial interpolation technique within the framework of the GIS-a fairly standard procedure for transforming point-based meteorological observations into continuous regional wind fields. This wind speed layer was then used later as the main driver in the assessment of wind erosion, because stronger winds have a greater potential to detach and transport soil particles. They are also found to be one of the main controls that determine the risk of aeolian erosion. (Figure 11).

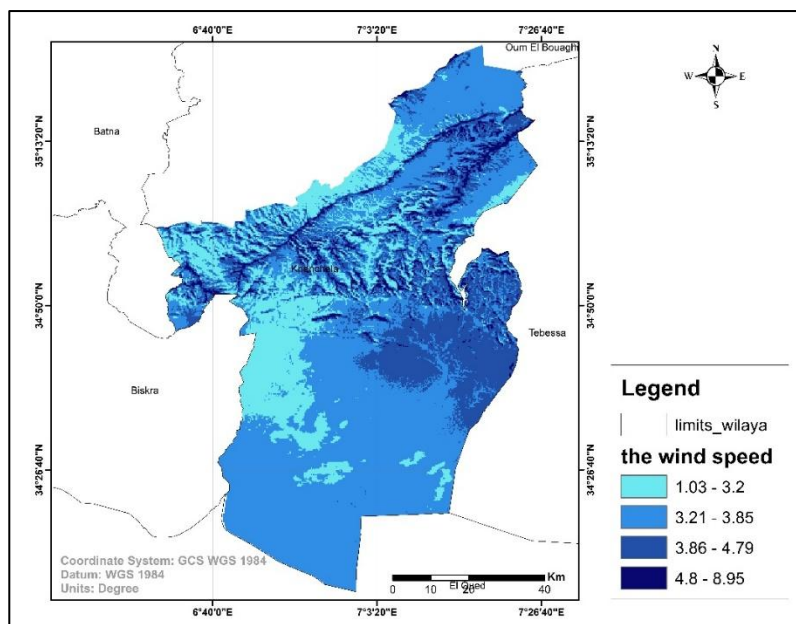


Figure 11. Wind speed map.

2.6.10 Population density

The demographic information was retrieved from the most recent national census and incorporated into the GIS database to represent the distribution of settlements within the study area. Two types of settlement pattern may be distinguished in the Nemamcha Mountains: settlements concentrated in the Aurès highland areas (Ammamras, for instance), and settlements in the Jebel Chechar area, which are mostly found in valleys and footslope areas. The differentiation of settlements according to their topography corresponds to local adaptation strategies. The density of the human population was included as a socio-economical factor in the model of wind erosion, considering that human impact, and specifically increased land use, is a well-recognized factor for land degradation and increased susceptibility to erosion in arid and semi-arid regions, in general (Geist and Lambin, 2004; Reynolds et al., 2007). Other studies involving susceptibility mapping through GIS, such as this study, must include anthropogenic parameters to accurately represent human impact contribution to the pattern of susceptibility to erosion, as well (Higginbottom and Symeonakis, 2014; Mihi and Benaradj, 2022). (Figure 12).

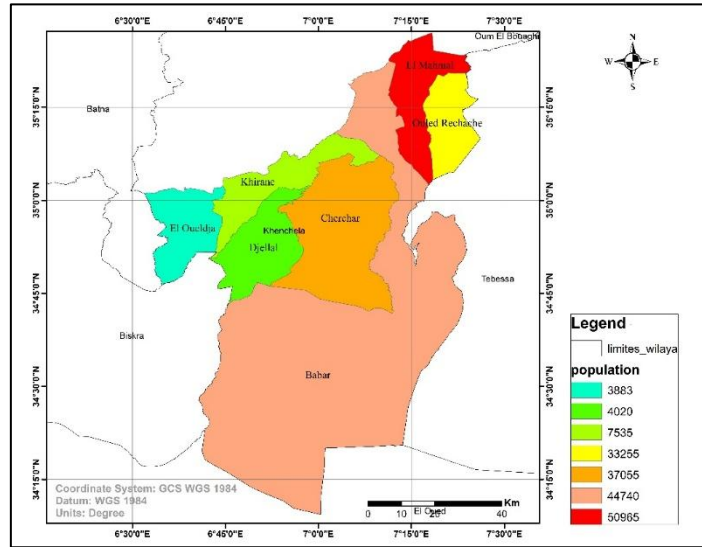


Figure 12. Population map.

2.6.11 Road network density

The road network map of southern Khenchela was produced through the compilation of available transport layers and digitization of the road infrastructure in a GIS environment. Roads were differentiated into hierarchical classes (main, secondary, tertiary) and also unpaved rural tracks connecting scattered settlements and were spatially integrated with administrative boundaries and built-up areas to improve positional consistency. The layer of the road network has been included as a socioeconomic factor, given that accessibility by roads is closely related to human disturbance, intensity of land use, and vegetation removal, which may accelerate land degradation and increase soil exposure to wind erosion. Various current publications indicate that the extension and densification of roads may lead to landscape degradation by increased human pressure and fragmentary effects. The spatial representation of road distribution is an important anthropogenic factor for the evaluation of erosion susceptibility within multi-criteria frameworks based on GIS. (Figure 13).

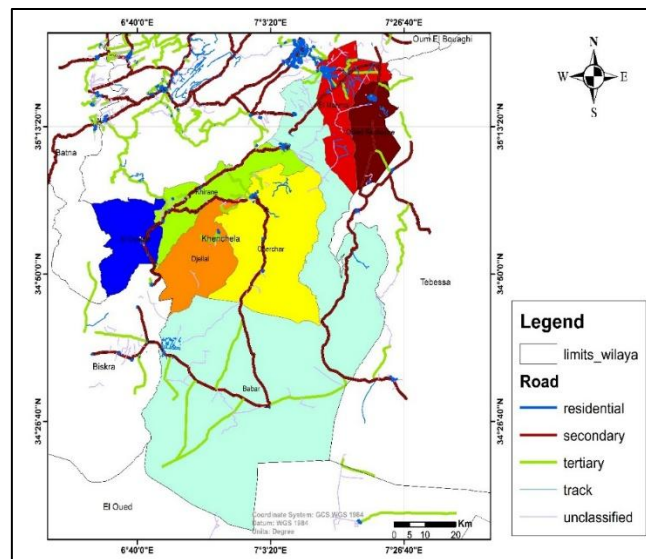


Figure 13. Road network density map.

3. Results

The final susceptibility index was produced using a multiplicative combination approach, in which four main groups of criteria were integrated: vegetation cover, socio-economic pressure, soil characteristics, and climatic conditions. This multi-criteria procedure using GIS is widely adopted for environmental susceptibility mapping, given its ability to integrate heterogeneous factors into a single spatial index.

The normalized output was then ranked and classified into classes ranging from 0 to 4, with larger pixels representing areas where wind erosion has a high potential. To make it easier for interpretation, this index was then converted into five risk classes regarding wind erosion (very low, low, moderate, high, and very high classes). Table 1 below highlights the surface covered by risk classes in hectares and percentages, respectively.

3.1 Spatial analysis

Spatial analysis of the wind erosion susceptibility map reveals that aeolian erosion is a widespread process in the Wilaya of Khenchela. The sectors in the northern and central parts seem to be the most exposed areas. Indeed, strong prevailing winds combined with low vegetation cover and sandy or weakly structured soils favor sediment detachment and transport in such sectors (Mihi and Benaradj, 2022). Conversely, it appears that relatively lower susceptibility generally characterizes the mountainous zones of the Aurès and Nemamcha ranges. Their denser vegetation cover and generally more stable conditions of topography would have reduced surface exposure and mobility of soil due to wind (Okin et al., 2006; Smyth et al., 2019).

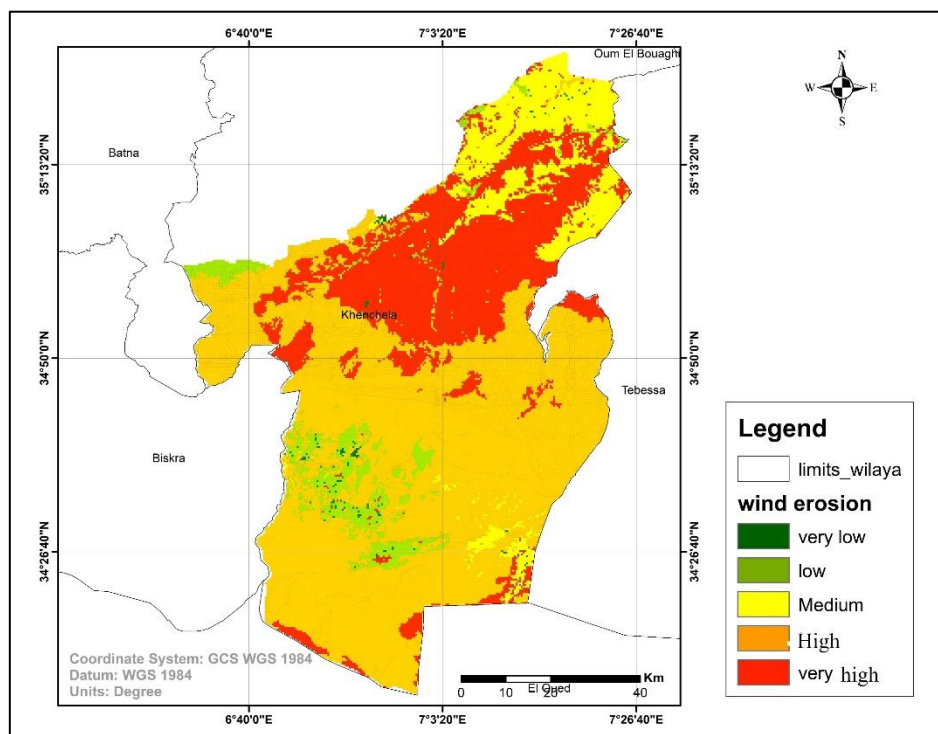


Figure 14. Map of wind erosion susceptibility classes.

Table 1. Area and percentage of erosion classes

Significance class of wind erosion	Number of pixels	The surface area in hectares	The surface area in %
Very low	161	2140.52	0.34
Low	2665	35444.46	5.63
Medium	5259	70007.52	11.12
High	27597	366972.89	58.29
Very high	11554	154998.66	24.62
Total	47236	629564.23	100

3.2 Susceptibility classes

3.2.1 Very high susceptibility class

The very high susceptibility class corresponds to the most affected areas, which are mainly located in the central part of the study area, especially around Chechar, Djellal, as well as the southern areas of Babar, especially Khiran. This class is characterized by the predominance of very fragile soils that have a light texture, in addition to the lack of vegetation cover. Such conditions, associated with low surface protection, make it easy for sediments to be mobilized under the effect of high wind forcing. Additionally, anthropogenic impact in the form of overgrazing as well as vegetation removal tends to accelerate land degradation through the reduction of surface roughness as well as the decrease in soil cohesion, thus facilitating the detachment as well as the transport of soil particles. Taken as a whole, the geographic distribution of this class corresponds to the combination of wind intensity, soil characteristics, lack of vegetation cover, as well as land use disturbance, factors that have been commonly reported in the literature as having a major controlling impact on aeolian erosion in semi-arid conditions (Sterk, 2003; Okin et al., 2006; Ravi et al., 2010; Mihi and Benaradj, 2022).

Sandy and dry soils are typically loose and weakly cohesive, which makes them highly vulnerable to wind action in arid and semi-arid regions.

Sparse vegetation cover, driven by climatic constraints and land-use disturbance, reduces surface roughness and increases soil exposure to wind erosion.

3.2.2 High susceptibility class

Areas classified as high erosion generally occur around the most degraded zones and form transitional belts between very high-risk areas and relatively more stable surfaces. Although less severely affected, these zones remain vulnerable, particularly in agricultural lands dominated by sandy to loamy soils. This vulnerability is mainly driven by frequent soil disturbance and the lack of protective surface cover, which increase soil exposure and accelerate degradation processes (Mihi and Benaradj, 2022). Therefore, mitigation measures such as the establishment of windbreaks, the use of vegetative barriers, and the adoption of conservation agriculture practices are strongly recommended to reduce near-surface wind velocity and limit sediment transport (Rehacek et al., 2017; Barrientos-Perez et al., 2023).

3.2.3 Moderate susceptibility class

The moderate susceptibility class is a transitional area between very degraded and relatively stable land. Vegetation density in these areas is generally moderate, commonly characterized by steppe vegetation such as *Stipa tenacissima*, or alpha grass, which partially shelters the topsoil and is an important factor in the land’s stabilization under arid conditions (Le Houérou, 2001).

Although these regions can currently be used for agricultural purposes, the implementation of sustainable agriculture practices such as crop rotation, minimum tillage agriculture, and agro-ecological farming systems is necessary in order to avoid further degradation and susceptibility to wind erosion.

3.2.4 Low susceptibility class

Regions that belong to the low erosion category have a higher density of vegetation and conditions that make it easier to travel, which increase the stability of the soils and make it less susceptible to aeolian forces of erosion. Vegetation is very important in inhibiting aeolian erosion by increasing the height of the terrain, which reduces the speed of the wind and its erosive power (Okin et al., 2006; Ravi et al., 2010).

Therefore, preserving such vegetation areas becomes very important in terms of ecosystem functioning, as well as in preventing the spread of the process of degradation.

3.2.5 Very low susceptibility class

Very low erosion class: Erosional rates in this class are minimal, while the rates of wind erosion are low, hence the formation of stable land. This class is found in regions of dense vegetation cover, as well as in valley bottoms. This is according to Okin et al. (2006).

They are still useful for agricultural use and land use with moderate constraints on erosion, but protecting the status quo of land use/land cover is vital for preventing damage from future climatic changes and land use practices (Ravi et al., 2010).

4. Discussion

The susceptibility map produced in this study shows a clear dominance of the high and very high classes (82.91% of the study area), indicating that aeolian erosion constitutes a major land degradation process in southern Khenchela. The spatial pattern displayed in Figure 14 highlights strong contrasts between exposed sectors and protected mountainous zones, which is consistent with the role of vegetation cover, soil texture, and wind regime as primary drivers of wind erosion in semi-arid environments (Sterk, 2003; Okin et al., 2006; Ravi et al., 2010).

The very large extent of the high class (58.29%) suggests that susceptibility is not limited to isolated hotspots but affects broad surfaces across the study region. The very high class (24.62%), concentrated mainly in central and southern sectors, indicates the presence of areas where susceptibility factors converge, producing the maximum susceptibility levels recorded by the index. By contrast, the combined proportion of low and very low classes (5.97%) remains limited, suggesting that truly protected surfaces represent only a small fraction of the study area.

The spatial organization of susceptibility classes supports widely documented controls of wind erosion in drylands. Areas mapped as high to very high susceptibility coincide with sectors where vegetation cover is reduced and soils are predominantly sandy to loamy. These surface conditions are commonly associated with lower aggregate stability and weaker cohesion of soil particles, making them easier to detach and transport under strong winds (Sterk, 2003; Okin et al., 2006). In contrast, lower susceptibility in mountainous areas of the Aurès and Nemamcha ranges reflects the protective contribution of denser vegetation and topographic sheltering (Okin et al., 2006; Smyth et al., 2019). The results are consistent with studies that applied GIS and remote sensing frameworks to identify aeolian erosion hotspots. In northeastern Morocco (Middle Moulouya Basin), Elyagoubi and Mezrhah (2022) reported that sandy to loamy soils combined with low vegetation cover and strong prevailing winds correspond to the most vulnerable zones. Similarly, Funk and Völker (2024), using the WERA GIS toolbox, identified sparse vegetation and light soil texture as key determinants of high susceptibility and highlighted the role of land-structure elements (e.g., tree belts and forest patches) in reducing susceptible surfaces.

Beyond climatic and soil controls, the susceptibility distribution also reflects areas of elevated socio-economic pressure. In semi-arid rangelands, overgrazing and vegetation removal reduce roughness elements and surface protection, increasing exposure to wind forcing (Ravi et al., 2010). In agricultural settings, frequent soil disturbance can maintain a loose surface layer and reduce vegetation cover during critical periods, contributing to higher susceptibility (Mihi and Benaradj, 2022).

From a management perspective, the susceptibility map provides a spatial basis for prioritizing mitigation. High and very high susceptibility zones should be considered priority targets for interventions that increase surface protection and reduce near-surface wind velocity. Measures reported as effective include windbreaks, vegetative barriers, and conservation-oriented practices (Rehacek et al., 2017; Barrientos-Perez et al., 2023). Moderate susceptibility areas should be managed to prevent transition toward higher susceptibility, while low and very low zones should be preserved.

Although the GIS-based multi-criteria approach is effective for integrating heterogeneous information into a single index, the resulting map remains dependent on the quality and resolution of input layers and on the weighting, scheme used in the multiplicative combination. Future work could strengthen the assessment through sensitivity testing of weights, comparison with field indicators of aeolian activity, and inclusion of land-structure elements when available (Funk and Völker, 2024).

5. Conclusion

In this study, a GIS-based multi-criteria analysis method was adopted to delineate wind erosion susceptibility maps of the Nemamcha region. The parameters of climate, soils, topography, as well as current land use, have been taken into consideration. The method adopted in this study has therefore succeeded in identifying areas liable to wind erosion. In this regard, more than 80% of the study region remains categorized as moderately to highly vulnerable to wind erosion, with the areas of vital concern located from the center to the southern region around Chechar, Djellal, and Babar. The region highly vulnerable to wind erosion is characterized by the primary attributes of sandy soils, a lack of vegetation, as well as dominant prevailing winds.

Conversely, vegetation density and topographic factors that are more stable showed lower susceptibility to wind erosion, pinpointing the ameliorating effects of vegetation and topographic stability in fighting wind erosion. In summation, these results have verified that the contributing factors that determine wind erosion in semi-arid conditions are indeed vegetation density, soil type, and wind force dynamics.

Integration of remote sensing techniques and GIS analysis capabilities appeared to be useful in the mapping of erosion sensitivity. In efforts to ensure the long-term sustainability of the land, it would be recommended that reforestation, controlled grazing, establishment of windbreaks, and the development of green barriers be encouraged, especially in the high-risk areas. Further refinement in the modeling of erosion, taking into account other factors such as landscape characteristics, soil moisture, as well as land management practices, should be explored in future research.

6. Statements and declarations

6.1 Funding

This research did not receive any specific grant from funding agencies in the public, commercial, or not-for-profit sectors.

6.2 Competing interests

The authors declare that they have no known competing financial interests or personal relationships that could have appeared to influence the work reported in this paper.

6.3 Ethical approval

This study did not involve human participants or animals and therefore did not require ethical approval.

6.4 Data availability

The datasets generated and analyzed during the current study are available from the corresponding author on reasonable request.

7. References

- [1] Assami, T., & Hamdi-Aissa, B. (2019). Digital mapping of soil classes in Algeria-A comparison of methods. *Geoderma Regional*, 16, e00215. <https://doi.org/10.1016/j.geodrs.2018.e00215>
- [2] Barrientos-Perez, E., Carevic-Vergara, F. S., Rodriguez, J. P., Arenas-Charlin, J., & Delatorre-Herrera, J. (2023). Effect of native vegetative barriers to prevent wind erosion: A sustainable alternative for quinoa

- (Chenopodium quinoa Willd.) production. *Agriculture*, 13(7), 1432. <https://doi.org/10.3390/agriculture13071432>
- [3] Bouajila, A., Omar, Z., Ajjari, A., Bol, R., & Brahim, N. (2022). Improved estimation and prediction of the wind-erodible fraction for Aridisols in arid southeast Tunisia. *Catena*, 211, 106001. <https://doi.org/10.1016/j.catena.2021.106001>
- [4] Colazo, J. C., & Buschiazzo, D. E. (2015). The impact of agriculture on soil texture due to wind erosion. *Land Degradation & Development*, 26(1), 62-70. <https://doi.org/10.1002/ldr.2297>
- [5] Congalton, R. G. (1991). A review of assessing the accuracy of classifications of remotely sensed data. *Remote Sensing of Environment*, 37(1), 35-46. [https://doi.org/10.1016/0034-4257\(91\)90048-B](https://doi.org/10.1016/0034-4257(91)90048-B)
- [6] Djeddaoui, F., Chadli, M., & Gloaguen, R. (2017). Desertification susceptibility mapping using logistic regression analysis in the Djelfa area, Algeria. *Remote Sensing*, 9(10), 1031. <https://doi.org/10.3390/rs9101031>
- [7] Djilali, B., Hartani, A., Aibout, F., Benaradj, A., Chouieb, M., & Mederbal, K. (2016). A GIS for the characterization and mapping of saline soils in semi-arid areas: Case of Oued Mina watershed (North West Algeria). *Journal of Biodiversity and Environmental Sciences*, 9(1), 410-419.
- [8] Elyagoubi, S., & Mezrhab, A. (2022). Using GIS and remote sensing for mapping land sensitivity to wind erosion hazard in the Middle Moulouya Basin (North-Eastern Morocco). *Journal of Arid Environments*, 202, 104753. <https://doi.org/10.1016/j.jaridenv.2022.104753>
- [9] Fensholt, R., & Sandholt, I. (2003). Derivation of a shortwave infrared water stress index from MODIS near- and shortwave infrared data. *Remote Sensing of Environment*, 87, 111-121. <https://doi.org/10.1016/j.rse.2003.07.002>
- [10] Fenta, A. A., Tsunekawa, A., Haregeweyn, N., Poesen, J., Tsubo, M., Borrelli, P., ... & Kurosaki, Y. (2020). Land susceptibility to water and wind erosion risks in the East Africa region. *Science of the Total Environment*, 703, 135016. <https://doi.org/10.1016/j.scitotenv.2019.135016>
- [11] Foody, G. M. (2002). Status of land cover classification accuracy assessment. *Remote Sensing of Environment*, 80(1), 185-201. [https://doi.org/10.1016/S0034-4257\(01\)00295-4](https://doi.org/10.1016/S0034-4257(01)00295-4)
- [12] Funk, R., & Völker, L. (2024). A GIS-toolbox for a landscape structure based Wind Erosion Risk Assessment (WERA). *MethodsX*, 13, 103006. <https://doi.org/10.1016/j.mex.2024.103006>
- [13] Gao, B.-C. (1996). NDWI-A normalized difference water index for remote sensing of vegetation liquid water. *Remote Sensing of Environment*, 58, 257-266. [https://doi.org/10.1016/S0034-4257\(96\)00067-3](https://doi.org/10.1016/S0034-4257(96)00067-3)
- [14] Geist, H. J., & Lambin, E. F. (2004). Dynamic causal patterns of desertification. *BioScience*, 54(9), 817-829. [https://doi.org/10.1641/0006-3568\(2004\)054\[0817:DCPOD\]2.0.CO;2](https://doi.org/10.1641/0006-3568(2004)054[0817:DCPOD]2.0.CO;2)
- [15] Ghosal, K., & Das Bhattacharya, S. (2020). A review of RUSLE model. *Journal of the Indian Society of Remote Sensing*, 48(4), 689-707. <https://doi.org/10.1007/s12524-019-01097-0>
- [16] Hagen, L. J. (2004). Evaluation of the Wind Erosion Prediction System (WEPS) erosion submodel on cropland fields. *Environmental Modelling & Software*, 19(2), 171-176. [https://doi.org/10.1016/S1364-8152\(03\)00119-1](https://doi.org/10.1016/S1364-8152(03)00119-1)
- [17] Higginbottom, T. P., & Symeonakis, E. (2014). Assessing land degradation and desertification using vegetation index data: Current frameworks and future directions. *Remote Sensing*, 6(10), 9552-9575. <https://doi.org/10.3390/rs6109552>
- [18] Lal, R. (2003). Soil erosion and the global carbon budget. *Environment International*, 29(4), 437-450. [https://doi.org/10.1016/S0160-4120\(02\)00192-7](https://doi.org/10.1016/S0160-4120(02)00192-7)
- [19] Le Houerou, H. N. (2001). Biogeography of the arid steppeland north of the Sahara. *Journal of Arid Environments*, 48(2), 103-128. <https://doi.org/10.1006/jare.2000.0679>
- [20] Lyles, L., & Tatarko, J. (1986). Wind erosion effects on soil texture and organic matter. *Journal of Soil and Water Conservation*, 41, 191-193. <https://doi.org/10.1080/00224561.1986.12455968>
- [21] Malczewski, J. (2006). GIS-based multicriteria decision analysis: A survey of the literature. *International Journal of Geographical Information Science*, 20(7), 703-726. <https://doi.org/10.1080/13658810600661508>

- [22] Mihi, A., & Benaradj, A. (2022). Assessing and mapping wind erosion-prone areas in Northeastern Algeria using additive linear model, fuzzy logic, multicriteria, GIS, and remote sensing. *Environmental Earth Sciences*, 81, 47. <https://doi.org/10.1007/s12665-021-10154-2>
- [23] Okin, G. S., Gillette, D. A., & Herrick, J. E. (2006). Multi-scale controls on and consequences of aeolian processes in landscape change in arid and semi-arid environments. *Journal of Arid Environments*, 65(2), 253-275. <https://doi.org/10.1016/j.jaridenv.2005.06.029>
- [24] Pal, M., & Mather, P. M. (2003). An assessment of the effectiveness of decision tree methods for land cover classification. *Remote Sensing of Environment*, 86(4), 554-565. [https://doi.org/10.1016/S0034-4257\(03\)00132-9](https://doi.org/10.1016/S0034-4257(03)00132-9)
- [25] Pettorelli, N., Vik, J. O., Mysterud, A., Gaillard, J.-M., Tucker, C. J., & Stenseth, N. C. (2005). Using the satellite-derived NDVI to assess ecological responses to environmental change. *Trends in Ecology & Evolution*, 20(9), 503-510. <https://doi.org/10.1016/j.tree.2005.05.011>
- [26] Ravi, S., Breshears, D. D., Huxman, T. E., & D'Odorico, P. (2010). Land degradation in drylands: interactions among hydrologic–aeolian erosion and vegetation dynamics. *Geomorphology*, 116(3-4), 236-245. <https://doi.org/10.1016/j.geomorph.2009.11.023>
- [27] Rehacek, D., Khel, T., Kucera, J., Vopravil, J., & Petera, M. (2017). Effect of windbreaks on wind speed reduction and soil protection against wind erosion. *Soil and Water Research*, 12, 128-135. <https://doi.org/10.17221/45/2016-SWR>
- [28] Reynolds, J. F., Stafford Smith, D. M., Lambin, E. F., et al. (2007). Global desertification: Building a science for dryland development. *Science*, 316(5826), 847-851. <https://doi.org/10.1126/science.1131634>
- [29] Roy, D. P., Wulder, M. A., Loveland, T. R., et al. (2014). Landsat-8: Science and product vision for terrestrial global change research. *Remote Sensing of Environment*, 145, 154-172. <https://doi.org/10.1016/j.rse.2014.02.001>
- [30] Smyth, T. A. G., Hesp, P. A., Walker, I. J., Wasklewicz, T., Gares, P. A., & Smith, A. B. (2019). Topographic change and numerically modelled near-surface wind flow in a bowl blowout. *Earth Surface Processes and Landforms*, 44, 1064-1076. <https://doi.org/10.1002/esp.4625>
- [31] Sterk, G. (2003). Causes, consequences and control of wind erosion in Sahelian Africa: A review. *Land Degradation & Development*, 14(1), 95-108. <https://doi.org/10.1002/ldr.526>
- [32] Tucker, C. J. (1979). Red and photographic infrared linear combinations for monitoring vegetation. *Remote Sensing of Environment*, 8(2), 127-150. [https://doi.org/10.1016/0034-4257\(79\)90013-0](https://doi.org/10.1016/0034-4257(79)90013-0)